Polyamide thin-film composite membranes based on carboxylated polysulfone microporous support membranes for forward osmosis

Cho, Young Hoon; Han, Jungim; Han, Sungsoo; Guiver, Michael D.; Park, Ho Bum

Publisher's version / Version de l'éditeur:
https://doi.org/10.1016/j.memsci.2013.06.003
Journal of Membrane Science, 445, pp. 220-227, 2013-06-13

Polyamide Thin-Film Composite Membranes Based on Carboxylated Polysulfone Microporous Support Membranes for Forward Osmosis

Young Hoon Cho[1], Jungim Han[2], Sungsoo Han[2], Michael D. Guiver[1,3] and Ho Bum Park[1,*]

[1]Hanyang University, WCU Department of Energy Engineering, Seoul, 133-791, Korea

[2] Samsung Advanced Institute of Technologies, Suwon, 440-600, Korea

[3] National Research Council Canada, Ottawa, ON, K1A 0R6, Canada

*Corresponding author (Tel: +82-2-2220-2338; Email: badtzhb@hanyang.ac.kr)

Manuscript prepared as a full paper in *Journal of Membrane Science*

Abstract

Due to its simple process and low energy consumption, forward osmosis (FO) has gained significant attention in the fields of emergency drinks, desalination, landfill leachate treatment, and brine concentration. However, current state-of-the-art reverse osmosis (RO) membranes show relatively low water fluxes in FO processes due to high internal concentration polarization (ICP) and high mass transfer resistance in commercially available microporous support membranes. In this study, carboxylated polysulfones (CPSFs) were synthesized via direct polysulfone (PSF) functionalization and considered as moderately hydrophilic, mechanically stable microporous support membranes. The incorporation of hydrophilic groups into hydrophobic polymer backbones often reduces mechanical strength due to excessive water swelling. However, the mechanical properties of CPSFs (degree of substitution, DS=0.45~0.85) were similar to those of pristine PSF, and they retained their hydrophilic nature. Microporous CPSF membranes were prepared in various conditions, and FO water fluxes and salt passages of polyamide thin-film/CPSF composite membranes were measured and compared with each other. CPSF-based FO membranes showed significantly higher water fluxes than PSF-based FO membranes at the same membrane formation conditions, which might be due to enhanced hydrophilicity and reduced ICP.

Keywords: Forward osmosis; Microporous Membrane; Desalination; Carboxylated Polysulfone

1. Introduction

Polyamide thin-film composite (PA TFC) membranes, which are mostly used as reverse osmosis (RO) membranes, consist of selective, thin polyamide layers and microporous support membranes [1]. These membranes dominate the current RO market (>95%) because of their high flux and salt rejection compared with cellulose-based RO membranes. Forward osmosis (FO) has recently been highlighted because of its many advantages, including reduced energy requirements [2, 3]. FO principally operates due to net osmotic pressure caused by differences in the water and salt activities between the feed and draw solutions. This is unlike RO, which requires high external pressure to overcome osmotic pressure. If proper techniques to separate water from draw solution are developed, FO membrane processes will be promising for desalination technology. New FO membranes have been extensively developed, but many studies have focused solely on the chemical and physical modification of conventional RO membranes, such as PA TFC membranes [4-6] and cellulosic membranes [7-9]. During the last decade, numerous membranes have been evaluated for FO membrane processes, and the key factors that affect FO performance have been studied to develop new FO membranes [10-14]. Ideally, an ultrathin semipermeable membrane that allows only water molecules (e.g., porous graphene) is preferred to maintain the net osmotic pressure between the feed and draw solutions [15]. Practically, such membranes cannot be used at all. Mechanically strong microporous support membranes with selective, thin layers in the form of composite or asymmetric membranes should be pursued for practical applications.

PA TFC membranes have been largely studied for FO membrane processes. However, PA TFC membranes exhibit some drawbacks, including low (reverse) salt passage from the draw solution (high salt concentration) to the feed solution (low salt concentration). The

primary problem is low water flux, which is caused by a net osmotic pressure difference across the membrane that is significantly lower than the theoretical osmotic pressure [16]. This phenomenon occurs mainly because of internal concentration polarization (ICP) due to microporous support membrane structures or wettability [17].

Hydrophilic surface or bulk modifications have been extensively investigated to overcome the low water flux and fouling problems of hydrophobic polysulfone (PSF) membranes [18, 19]. Chemical modifications, such as amination [20-22], sulfonation [23-25], and carboxylation [26-28], have been used to impart hydrophilicity to hydrophobic PSF. Sulfonated polysulfone (SPSF), mainly prepared by the post-sulfonation method, has been used for chlorine-tolerant RO membranes [29, 30]. However, it was withdrawn from the market due to limited solubility in common solvents and difficultly in controlling the degree of sulfonation. High sulfonation degrees are favorable, but can lead to excessive water swelling followed by mechanical failure. Chemically and physically stable SPSF was recently developed via a direct polycondensation reaction between sulfonated monomers and other monomers [31]. This process showed high chlorine tolerance and high salt rejection [32]. However, SPSF is still difficult to use for preparing thin-film composites or asymmetric microporous membranes because of problems mentioned above. For these reasons, carboxylated PSF (CPSF), which is considered to be a moderately hydrophilic, microporous support membrane, was used to prepare PA TFC composite membranes for FO in this work. Weak acid groups, such as carboxylic acid, differ from strong acid groups such as sulfonic acid, so that the polymer will not suffer from severe water swelling, even at a high ion exchange capacity (IEC). If the degree of substitution (DS) is properly controlled, this process provides a hydrophobic polymer with moderate hydrophilicity.

In this study, carboxylated polysulfones (CPSFs) were synthesized as supporting

membrane materials for FO membranes. Previously, Guiver *et al.* [26] reported the carboxylation of polysulfone (PSF) via a direct lithiation method followed by carbon dioxide and acid treatment. The chemical [26, 33, 34] and separation properties of these materials as RO and UF membranes [27, 28] have been reported in the literature. Here, CPSFs were prepared as new supporting membrane materials for FO membranes. Carboxylic acid groups in CPSF can improve the wettability of hydrophobic PSF [26]. The mechanical properties, water affinity, and membrane formation structure of CPSF were examined to elucidate its potential application as a new FO membrane. Here, FO membranes were prepared via interfacial polymerization of polyamide thin-film on PSF (as a control) and CPSF support layers. In addition, the correlation between support layer properties and FO performance is discussed in detail.

2. Experimental

2.1. Synthesis of carboxylated polysulfone (CPSF) and CPSF dense membranes

The synthesis procedure for CPSF is schematically illustrated in Fig. 1. [26]. A specific amount of *n*-butyllithium was added drop-wise to 10 wt/vol% PSF solution in THF at -50°C. After the lithiation procedure, excess CO_2 dry ice was added to the reaction mixture. The precipitated lithium salt form (PSF-COOLi) of the polymer was washed with ethanol. The acid form of the polymer (PSF-COOH) was then obtained by reaction with dilute hydrochloric acid. The final product was dried and stored in a vacuum oven at 60°C until membrane preparation. The degree of substitution (DS) (carboxyl groups per repeat unit) was changed from 0.45 to 0.85 via molar ratios of *n*-butyllithium and polysulfone.

CPSF polymer powders were dissolved in dimethylacetamide (DMAc) at 20 wt% and stirred overnight to obtain a homogeneous cast solution. The prepared dope solution was

thoroughly degassed in a sonication bath and stored at 5°C to remove residual air bubbles before membrane casting. The dope solutions were cast on clean glass plates and placed in a 60°C oven overnight. The temperature increased stepwise up to 120°C, and a vacuum was then applied for 12 hours to prepare the CPSF dense membranes. After natural cooling, CPSF dense membranes were rinsed to eliminate residual solvent and stored in deionized water for 24 hours. The CPSF membranes were stored and dried in a 60°C vacuum oven for 48 hours before characterizations.

2.2. Preparation of PSF and CPSF microporous support layers

PSF and CPSF were dissolved in common organic solvents (*i.e.*, dimethylformamide (DMF), DMAc) at 15 wt% and stirred overnight. Degassed dope solutions were cast on the clean glass plate using a thickness adjustable doctor knife (100-200 μm). After membrane casting, the phase inversion process was performed in a 25°C water bath. As a result, microporous PSF and CPSF membranes were successfully prepared. The microporous PSF and CPSF membranes were completely washed and stored in water before use.

2.3. Membrane characterizations

The mechanical properties of PSF and CPSF dense membranes were measured using a universal testing machine (AGS-J-500N, Shimadzu, Kyoto, Japan). To compare the mechanical properties of CPSF in dry and wet states, hydrated membranes were also prepared by immersing CPSF membranes in deionized water for 48 hours. The dry and wet membranes were cut into test coupons (2×13 mm^2) using customized cutting equipment. The effective membrane thickness was measured using a hand-held thickness gauge (Absolute 547-401, Mitutoyo, Kawasaki, Japan). Tensile strength (MPa) and elongation at maximum

stress (%) were measured from the average values of five samples.

Membrane samples were stored in deionized water for 48 hours to measure water uptake and membrane porosity. After sufficient soaking, the weight of wet polymer membranes was measured after wiping to remove excessive water droplets on the membrane surface. Water uptake was calculated from the ratio of absorbed water and polymer in the dry state as follows:

$$\text{Water uptake (\%)} = \frac{w_{wet} - w_{dry}}{w_{dry}} \times 100 \quad (1)$$

where w_{wet} and w_{dry} are the weight of polymer in wet and dry states, respectively. The average porosities of porous membranes were calculated from the equation below [6],

$$\text{Average porosity (\%)} = \frac{(w_{wet} - w_{dry}) / \rho_{water}}{(w_{wet} - w_{dry}) / \rho_{water} + w_{dry} / \rho_{polymer}} \times 100 \quad (2)$$

where ρ_{water} and $\rho_{polymer}$ are the densities of water (1 g/ml) and polymer, respectively. The densities of PSF and CPSF were measured using a top-loading electronic balance (XP205, Mettler-Toledo, Switzerland) coupled with a density kit.

Attenuated total reflectance – infrared (ATR-IR) spectroscopy (Nicolet 6700 FT-IR spectrometer, Thermo scientific, Marietta, OH, USA) and X-ray photoelectron spectroscopy (XPS) (Quantum 2000, Physical electronics, Chanhassen, MN, USA) were used to analyze the surface composition of CPSF dense and microporous membranes. The contact angle of membrane samples was measured using a contact angle instrument (Pheonix 300, SEO, Suwon, Korea). Dried membrane samples were placed on a flat plate, and the same volume of water was dropped from a syringe onto each sample. Contact angle images were taken immediately, and contact angle values were averaged from five different locations.

The cross-sectional morphologies of prepared microporous membranes were

observed using field-emission scanning electron microscopy (Thermal FE-SEM, JSM-700F, JEOL, Tokyo, Japan). To observe the cross-section morphologies, wet membrane samples were freeze-fractured in liquid nitrogen and dried. The images were taken at a resolution of ×1,000.

The hydraulic water fluxes of microporous PSF and CPSF membranes were measured by dead-end filtration. Deionized water was continuously fed to the stirred filtration cell (Amicon 8050, Millipore, Billerica, MA, USA) at a feed pressure of 1 bar using a N_2 cylinder. The permeated water was automatically weighed using a digital mass balance (PAG4102C, Ohaus, Parsippany, NJ, USA) connected to a personal computer, which was used to calculate water flux.

2.4. Polyamide (PA) thin-film-CPSF composite membranes

For the FO experiment, polyamide (PA) thin-film composite (TFC) membranes were prepared by interfacial polymerization on previously prepared microporous membranes. The microporous CPSF membranes were placed on an acryl plate with a glass frame, and 3 wt% aqueous *m*-phenylenediamine (MPD) solution was then poured on the microporous membrane surface. After soaking for 3 min, the MPD solution was removed and excessive droplets were wiped from the membrane surface with a rubber roller. Trimesoylchloride (TMC) solution in dodecane (0.1 wt/vol%) was immediately poured on the membrane surface, and a polyamide thin-layer immediately formed on microporous CPSF membranes. After allowing sufficient time for interfacial polymerization, the TMC solution was removed. The resultant PA-TFC membranes were rinsed several times with hexane and isopropanol, and then stored in deionized water until use.

2.5. Forward osmosis (FO) measurement

Water flux and salt passage through the PA-TFC membranes in FO mode were measured with lab-built cross-flow FO equipment. The membranes were placed into a membrane cell (effective membrane area = 42 cm^2) with the active layer facing feed solution in FO mode, and facing draw solution in pressure-retarded osmosis (PRO) mode. Deionized water and 1 M $MgCl_2$ were used as feed and draw solutions, respectively. The cross-flow rate was fixed at 1.5 LPM (liter per minute), and there was no external hydraulic pressure ($\Delta P = 0$) for both feed and draw solutions. Weight and conductivity changes were monitored and automatically recorded by a digital mass balance (PAG4102, Ohaus, Parsippany, NJ, USA) and conductivity meter (inoLab 720, WTW, Weilheim, Germany), respectively. The water flux and salt passage in both FO and PRO modes were calculated using the following equation,

$$J_W = \frac{\Delta w_{feed} \cdot \rho_w}{A \Delta t} \ (\mathrm{L/m^2 \cdot h}) \tag{3}$$

$$J_S = \frac{\Delta c_f \cdot V_f}{A \cdot \Delta t} \ (\mathrm{g/m^2 \cdot h}) \tag{4}$$

where J_W is the water flux, Δw_{feed} is the weight change of feed solution, ρ_w is the density of water (approx. = 1 g/ml), A is the membrane area, J_S is the salt passage, Δc_f is the concentration change of feed solution, and V_f is the volume of feed solution.

3. Results and Discussion

3.1. Effect of carboxylation on membrane properties

Hydrophilic modified FO membranes generally show greatly improved FO water fluxes because the hydrophilic nature of microporous support layers can alleviate the ICP effect by increasing water and salt diffusivities in the support layer [17, 35]. However, the

methods of hydrophilic modification of polymers (*e.g.*, grafting, blending, and copolymerization with hydrophilic moieties) often lead to mechanical failure due to excessive swelling in a hydrated state [36]. The mechanical properties of CPSF dense membranes are compared with those of dense PSF membrane in Fig. 2 (a). The tensile strength of dense membranes slightly decreases with increasing DS in both dry and wet state CPSFs. Carboxylic acid groups on PSF backbones slightly reduce the tensile strength, since such polar groups increase the chain stiffness and packing density of the amorphous PSF. These groups also reduce the flexibility of the polymer chain by contributing to thermal motion. Conversely, the mechanical strength of CPSF is much higher than that of sulfonated polysulfone (SPSF) with a similar DS [28]. In addition, the mechanical strength of CPSF in the wet state is not greatly reduced, since swelling is not significant.

The water uptake of CPSF dense membranes is shown in Figure 2 (b). The introduction of carboxylic acid groups improves the water affinity of hydrophobic PSF membranes, since polar functional groups such as hydroxyl, carboxylic acid, and sulfonic acid groups can interact with water via hydrogen bonding. After PSF carboxylation, water uptake increases with increasing DS from 0.93% (DS=0) to 3% (DS=0.85). The acidity of carboxylic acid groups is lower than that of sulfonic acid groups, and carboxylic acids usually exist as dimeric pairs due to their tendency to "self-associate" via hydrogen bonding [37]. For these reasons, CPSF exhibits lower water uptake than sulfonated polymers at similar ion exchange capacity (IEC) [36, 38].

The water swelling behavior of polymers also affects the mechanical strength of microporous membranes prepared by phase inversion processes. In general, membranes used for water purification and desalination should be mechanically stable and maintain a porous structure in aqueous environments. Excessive swelling of hydrophilic membrane materials

often causes pore shrinkage (i.e., swelling of pore walls), membrane breakage, and poor membrane performance. Highly swollen polymers are not suitable as support membrane materials, and other techniques are needed to retain mechanical stability even with high water affinity.

The contact angles and surface zeta potential of microporous CPSF membranes are shown in Fig. 3. The contact angle of the microporous CPSF membrane surface is lower than that of PSF membrane, indicating better wettability. Conversely, the contact angles of CPSF membranes increased with increased DS from 0.49 to 0.85. That is, wettability was reduced with higher DS. Figure 4 shows that the surface concentration of carboxyl groups on the membrane surface linearly increases with DS. In non-solvent (water)-induced phase separation processes, the porous membrane dense surface is formed in contact with water. Hydrophilic parts are mainly located on the membrane surface due to hydrophilic interactions with water. Therefore, carboxylic acid groups tend to move on the membrane surface. Although the surface concentration of carboxylic acid groups increases with DS, the surface contact angle also increases with DS in CPSF porous membranes. Such trends in the contact angles of microporous CPSF membranes correlate with that of the surface streaming zeta potential of CPSF at pH 6 [33]. The zeta potentials of the porous CPSF membranes at pH 6 are also presented in Fig. 3 for comparison. The dissociation of carboxylic acid groups might affect the surface charge density of CPSF. Therefore, the surface charge of CPSF in acid form is more negative at lower DS ranges. However, the surfaces of CPSF membranes with high DS will be swollen with water [33]. As a result, the electrokinetic shear plane moves far from the membrane surface, resulting in reduced membrane surface potential. The reduced surface charge density with high DS CPSFs increases the contact angle of the membrane surface.

3.2. Structures of CPSF membranes

A ternary phase diagram of different CPSF/solvent/water mixtures can be found in the literature [34]. The solubilities of CPSF in various organic solvents are similar to those of PSF. Water content at the cloud point increases with increasing DS in CPSF due to enhanced hydrophilicity caused by more carboxylic acid groups. As shown in Fig. 5, sponge-like structures mainly appear in microporous CPSF membranes due to slightly delayed demixing. The straight finger-like macrovoids in CPSF/DMAc membranes disappear, since the cloud point of CPSF in polymer/solvent/water systems is higher than PSF, as seen in the ternary phase diagram of CPSF [34]. However, macrovoid formation again occurs at high DS CPSF (0.85) in both DMAc and DMF-induced microporous membranes. With increasing hydrophilicity, the chemical affinity between water and polymer is more favorable. As a result, large macrovoids form due to the swelling of coagulated polymer.

The structural parameters of the support layer (i.e., porosity, tortuosity, and thickness) severely affect the transport of water and salt in FO membranes. The average porosities and thicknesses of PSF and CPSF membranes are shown in Fig. 6 (a). Both porosity and thickness tend to increase with DS due to membrane swelling in phase inversion processes. The average structure parameters of PSF and CPSF membranes calculated from average porosity, theoretical tortuosity ($\tau = 1 - \ln \varepsilon^2$) [39], and thickness are shown in Fig. 6 (b). The structural mass transfer resistances of CPSF membranes are higher than those of PSF membranes, with the exception of low DS CPSF (0.49). This is because thickness generally has a greater effect on structure parameters than porosity.

The pure water fluxes of PSF and CPSF support layers under hydraulic pressure are shown in Table 1 along with the water fluxes of their PA-TFC membranes in FO and PRO modes. The water fluxes of hydrophilic CPSF support membranes are over four times higher

than those of PSF support membranes. Since water permeation through porous substrates is strongly affected by membrane porosity, pore size, tortuosity, thickness, and hydrophilicity [40], the relative mass transfer resistance in support membranes is estimated by hydraulic water flux. CPSF (DS = 0.45) showed the highest water flux among CPSF support membranes, but water flux decreased with DS, as the swelling of microporous CPSF membrane structures might reduce membrane pore size and increase overall membrane thickness.

3.3. Interfacial polymerization of polyamide on CPSF membranes

Interfacially polymerized PA active layers were formed on top of prepared PSF and CPSF support layers. In interfacial polymerization procedures, the support layers were soaked with a MPD/water solution. Adsorbed MPD molecules in the wet support layer diffused out and reacted with TMC to form a thin PA layer at the membrane and organic solvent interface. Although reactions between carboxylic acid and diamine do not occur in ambient conditions, carboxylic acid groups on the CPSF membrane surface interacted strongly with MPD monomers, resulting in delayed interfacial polymerization reactions. Therefore, control of PA layer formation is needed to prevent draw solute leakage and to sustain high water/salt selectivity.

Surface and cross-sectional SEM images of PA layers on PSF and CPSF membranes are shown in Fig. 7. PA layers (100-200 nm thick) were successfully formed on PSF porous substrates. PA layers on CPSF porous membranes have a relatively loose ridge and valley structure in the general interfacial polymerization reaction time (1 min.). As reaction time increases, more stable and dense PA layers (200-300 nm) were formed on CPSF membranes.

The effect of interfacial polymerization reaction time on the FO performance of PA-

CPSF TFC membranes is illustrated in Fig. 8. Salt passage strongly depends on the water/salt selectivity of the active layer. Salt passage dramatically decreased with increased reaction time for PA-CPSF TFC membranes. By increasing the interfacial polymerization reaction time, denser PA layers were formed due to increased amounts of amine monomers diffusing to the organic phase [41]. FO water flux did not change despite improved selectivity of the PA layer. Mass transfer resistance due to ICP in the support layer, rather than resistance of the active layer, is the main obstacle for water permeation. Because of this, the severe salt passage in high flux FO membranes can be effectively reduced by enhancing the selectivity of the active layer without sacrificing water flux.

3.4.FO performances of PA-CPSF TFC membranes

The FO performances of PA-CPSF TFC membranes are compared with those of PA-PSF TFC membranes in Fig. 9. Water fluxes in the FO and PRO modes increased with DS. Similar to the trend for the water flux of porous substrates, FO water flux decreased with highly substituted CPSF (DS = 0.85). FO water flux is generally much lower than the theoretical value (calculated from water permeability in RO mode) due to the ICP effect. If the support layer has a low mass transfer resistance for water and draw solute, water flux will increase due to the reduction in the ICP effect. PA-TFC membranes based on microporous CPSF membranes prepared from DMAc and DMF exhibited higher FO and PRO water flux than PSF-based TFC membranes due to decreased structural mass transfer resistance and improved hydrophilicity. The water flux differences between FO and PRO modes were less significant in PA-CPSF membranes due to lower water and solute transport resistance in microporous CPSF support membranes. However, FO water flux is lower for CPSF 0.85 (DS=0.85) membranes than for CPSF 0.6 (DS=0.6) membranes due to the membranes

swelling with water.

Draw solute passage generally increases along with water flux in FO and PRO modes, since a reduction in the ICP effect increases the effective concentration difference at the active layer. A strong trade-off relationship between FO water flux and draw solute retention ($1/J_s$) has been reported in the literature, as shown in Fig. 10. When water flux was increased by increasing the osmotic pressure of the draw solution or reducing the ICP effect, salt passage also increased. This effect was due to an increase in the concentration gradient between the inner and outer surface of the active layer (i.e., the driving force of salt diffusion). A more selective active layer is needed to reduce draw solute passage in high water flux FO membranes. In this study, PA-CPSF FO membranes exhibited both higher water flux and draw solute rejection properties than PA-PSF FO membranes and recently reported FO membranes [8, 42-45].

4. Conclusions

Various PA TFC membranes for FO applications were prepared using PSF and CPSF as support layer materials. PSF-based polymers have properties desirable for a membrane material, such as high mechanical, chemical, and thermal stability. Although the tensile strength of CPSF slightly decreased with increasing DS, it was still high enough to warrant preparing porous membranes with CPSF for FO applications. Due to their polarity, carboxylic acid groups in hydrophobic polysulfone increase the hydrophilicity of the polymer. The hydrophlilicity of CPSF affects the polymer-solvent-nonsolvent interactions that determine membrane structures. The membrane formation and structures of PSF and CPSF varied with organic solvent and DS. CPSF membranes are more favorable for a support layer for FO membranes than PSF membranes due to their high porosity and hydrophilicity. The FO water fluxes of CPSF-based membranes are higher than those of PSF-based membranes due to

hydrophilicity.

5. Acknowledgements

The World Class University (WCU) Program of the Ministry of Education, Science, and Technology (MEST) in Korea supported this study.

6. References

[1] K.P. Lee, T.C. Arnot, D. Mattia, A review of reverse osmosis membrane materials for desalination-Development to date and future potential, J. Membr. Sci., 370 (2011) 1-22.
[2] M. Elimelech, W.A. Phillip, The Future of Seawater Desalination: Energy, Technology, and the Environment, Science, 333 (2011) 712-717.
[3] T.Y. Cath, A.E. Childress, M. Elimelech, Forward osmosis: Principles, applications, and recent developments, J. Membr. Sci., 281 (2006) 70-87.
[4] N.Y. Yip, A. Tiraferri, W.A. Phillip, J.D. Schiffman, M. Elimelech, High Performance Thin-Film Composite Forward Osmosis Membrane, Environ. Sci. Technol., 44 (2010) 3812-3818.
[5] X.X. Song, Z.Y. Liu, D.R.D.L. Sun, Nano Gives the Answer: Breaking the Bottleneck of Internal Concentration Polarization with a Nanofiber Composite Forward Osmosis Membrane for a High Water Production Rate, Adv. Mater., 23 (2011) 3256-3260.
[6] J. Wei, C.Q. Qiu, C.Y.Y. Tang, R. Wang, A.G. Fane, Synthesis and characterization of flat-sheet thin film composite forward osmosis membranes, J. Membr. Sci., 372 (2011) 292-302.
[7] J.C. Su, Q. Yang, J.F. Teo, T.S. Chung, Cellulose acetate nanofiltration hollow fiber membranes for forward osmosis processes, J. Membr. Sci., 355 (2010) 36-44.
[8] K.Y. Wang, R.C. Ong, T.S. Chung, Double-Skinned Forward Osmosis Membranes for Reducing Internal Concentration Polarization within the Porous Sublayer, Ind. Eng. Chem. Res., 49 (2010) 4824-4831.
[9] S. Zhang, K.Y. Wang, T.S. Chung, H.M. Chen, Y.C. Jean, G. Amy, Well-constructed cellulose acetate membranes for forward osmosis: Minimized internal concentration polarization with an ultra-thin selective layer, J. Membr. Sci., 360 (2010) 522-535.
[10] W.Y. Li, Y.B. Gao, C.Y.Y. Tang, Network modeling for studying the effect of support structure on internal concentration polarization during forward osmosis: Model development and theoretical analysis with FEM, J. Membr. Sci., 379 (2011) 307-321.
[11] L. Shi, S.R. Chou, R. Wang, W.X. Fang, C.Y. Tang, A.G. Fane, Effect of substrate structure on the performance of thin-film composite forward osmosis hollow fiber membranes, J. Membr. Sci., 382 (2011) 116-123.
[12] W.L. Tang, H.Y. Ng, Concentration of brine by forward osmosis: Performance and influence of membrane structure, Desalination, 224 (2008) 143-153.
[13] M. Park, J.J. Lee, S. Lee, J.H. Kim, Determination of a constant membrane structure parameter in forward osmosis processes, J. Membr. Sci., 375 (2011) 241-248.
[14] A. Tiraferri, N.Y. Yip, W.A. Phillip, J.D. Schiffman, M. Elimelech, Relating performance of thin-film composite forward osmosis membranes to support layer formation and structure, J. Membr. Sci., 367 (2011) 340-352.

[15] D. Cohen-Tanugi, J.C. Grossman, Water Desalination across Nanoporous Graphene, Nano Lett., 12 (2012) 3602-3608.
[16] J.R. McCutcheon, M. Elimelech, Influence of concentrative and dilutive internal concentration polarization on flux behavior in forward osmosis, J Membr. Sci., 284 (2006) 237-247.
[17] J.R. McCutcheon, M. Elimelech, Influence of membrane support layer hydrophobicity on water flux in osmotically driven membrane processes, J. Membr. Sci., 318 (2008) 458-466.
[18] K.C. Khulbe, C. Feng, T. Matsuura, The Art of Surface Modification of Synthetic Polymeric Membranes, J. Appl. Polym. Sci., 115 (2010) 855-895.
[19] C.S. Zhao, J.M. Xue, F. Ran, S.D. Sun, Modification of polyethersulfone membranes - A review of methods, Prog. Mater. Sci., 58 (2013) 76-150.
[20] M. Rucka, G. Pozniak, B. Turkiewicz, W. Trochimczuk, Ultrafiltration membranes from polysulfone/aminated polysulfone blends with proteolytic activity, Enzyme Microb. Tech., 18 (1996) 477-481.
[21] D.L. Arockiasamy, A. Nagendran, K.H. Shobana, D. Mohan, Preparation and Characterization of Cellulose Acetate/Aminated Polysulfone Blend Ultrafiltration Membranes and their Application Studies, Separ. Sci. Technol., 44 (2009) 398-421.
[22] M.H. Chen, T.C. Chiao, T.W. Tseng, Preparation of sulfonated polysulfone/polysulfone and aminated polysulfone/polysulfone blend membranes, J. Appl. Polym. Sci., 61 (1996) 1205-1209.
[23] N. Vinnikova, G.B. Tanny, Transport of Ions and Water in Sulfonated Polysulfone Membranes, ACS Symposium Series, 153 (1981) 351-365.
[24] I. Jitsuhara, S. Kimura, Structure and Properties of Charged Ultrafiltration Membranes Made of Sulfonated Polysulfone, J. Chem. Eng. Jpn., 16 (1983) 389-393.
[25] R. Malaisamy, R. Mahendran, D. Mohan, M. Rajendran, V. Mohan, Cellulose acetate and sulfonated polysulfone blend ultrafiltration membranes. I. Preparation and characterization, J. Appl. Polym. Sci., 86 (2002) 1749-1761.
[26] M.D. Guiver, S. Croteau, J.D. Hazlett, O. Kutowy, Synthesis and Characterization of Carboxylated Polysulfones, Brit. Polym. J., 23 (1990) 29-39.
[27] M.D. Guiver, A.Y. Tremblay, C.M. Tam, Reverse-Osmosis Membranes from Novel Hydrophilic Polysulfones, Proceedings of the symposium on Advances in Reverse Osmosis and Ultrafiltration (1989) 53-70.
[28] D. Mockel, E. Staude, M.D. Guiver, Static protein adsorption, ultrafiltration behavior and cleanability of hydrophilized polysulfone membranes, J. Membr. Sci., 158 (1999) 63-75.
[29] A.E. Allegrezza, B.S. Parekh, P.L. Parise, E.J. Swiniarski, J.L. White, Chlorine Resistant Polysulfone Reverse-Osmosis Modules, Desalination, 64 (1987) 285-304.
[30] C. Brousse, R. Chapurlat, J.P. Quentin, New Membranes for Reverse-Osmosis .1. Characteristics of Base Polymer - Sulfonated Polysulfones, Desalination, 18 (1976) 137-153.
[31] F. Wang, M. Hickner, Q. Ji, W. Harrison, J. Mecham, T.A. Zawodzinski, J.E. McGrath, Synthesis of highly sulfonated poly(arylene ether sulfone) random (statistical) copolymers via direct polymerization, Macromol. Symp., 175 (2001) 387-395.
[32] H.B. Park, B.D. Freeman, Z.B. Zhang, M. Sankir, J.E. McGrath, Highly chlorine-tolerant polymers for desalination, Angew. Chem. Int. Edit., 47 (2008) 6019-6024.
[33] D. Mockel, E. Staude, M. Dal-Cin, K. Darcovich, M. Guiver, Tangential flow streaming potential measurements: Hydrodynamic cell characterization and zeta potentials of carboxylated polysulfone membranes, J. Membr. Sci., 145 (1998) 211-222.

[34] W.W.Y. Lau, M.D. Guiver, T. Matsuura, Phase-Separation in Carboxylated Polysulfone Solvent Water-Systems, Journal of Applied Polymer Science, 42 (1991) 3215-3221.
[35] J.T. Arena, B. McCloskey, B.D. Freeman, J.R. McCutcheon, Surface modification of thin film composite membrane support layers with polydopamine: Enabling use of reverse osmosis membranes in pressure retarded osmosis, J. Membr. Sci., 375 (2011) 55-62.
[36] R. Guan, H. Zou, D.P. Lu, C.L. Gong, Y.F. Liu, Polyethersulfone sulfonated by chlorosulfonic acid and its membrane characteristics, Eur. Polym. J., 41 (2005) 1554-1560.
[37] V. Doan, R. Koppe, P.H. Kasai, Dimerization of carboxylic acids and salts: An IR study in perfluoropolyether media, J. Am. Chem. Soc., 119 (1997) 9810-9815.
[38] F. Wang, M. Hickner, Y.S. Kim, T.A. Zawodzinski, J.E. McGrath, Direct polymerization of sulfonated poly(arylene ether sulfone) random (statistical) copolymers: candidates for new proton exchange membranes, J. Membr. Sci., 197 (2002) 231-242.
[39] B.P. Boudreau, The diffusive tortuosity of fine-grained unlithified sediments, Geochim. Cosmochim. Ac., 60 (1996) 3139-3142.
[40] J. Mulder, Basic Principles of Membrane Technology, 2nd ed., Springer, 1996.
[41] J. Lee, A. Hill, S. Kentish, Formation of a thick aromatic polyamide membrane by interfacial polymerisation, Sep. Purif. Technol., 104 (2013) 276-283.
[42] Q. Yang, K.Y. Wang, T.S. Chung, Dual-Layer Hollow Fibers with Enhanced Flux As Novel Forward Osmosis Membranes for Water Production, Environ. Sci. Technol., 43 (2009) 2800-2805.
[43] Q. Saren, C.Q. Qiu, C.Y.Y. Tang, Synthesis and Characterization of Novel Forward Osmosis Membranes based on Layer-by-Layer Assembly, Environ. Sci. Technol., 45 (2011) 5201-5208.
[44] L. Setiawan, R. Wang, K. Li, A.G. Fane, Fabrication of novel poly(amide-imide) forward osmosis hollow fiber membranes with a positively charged nanofiltration-like selective layer, J. Membr. Sci., 369 (2011) 196-205.
[45] S.R. Qi, C.Q. Qiu, Y. Zhao, C.Y.Y. Tang, Double-skinned forward osmosis membranes based on layer-by-layer assembly-FO performance and fouling behavior, J. Membr. Sci., 405 (2012) 20-29.
[46] N. Widjojo, T.S. Chung, M. Weber, C. Maletzko, V. Warzelhan, The role of sulphonated polymer and macrovoid-free structure in the support layer for thin-film composite (TFC) forward osmosis (FO) membranes, J. Membr. Sci., 383 (2011) 214-223.

List of figures

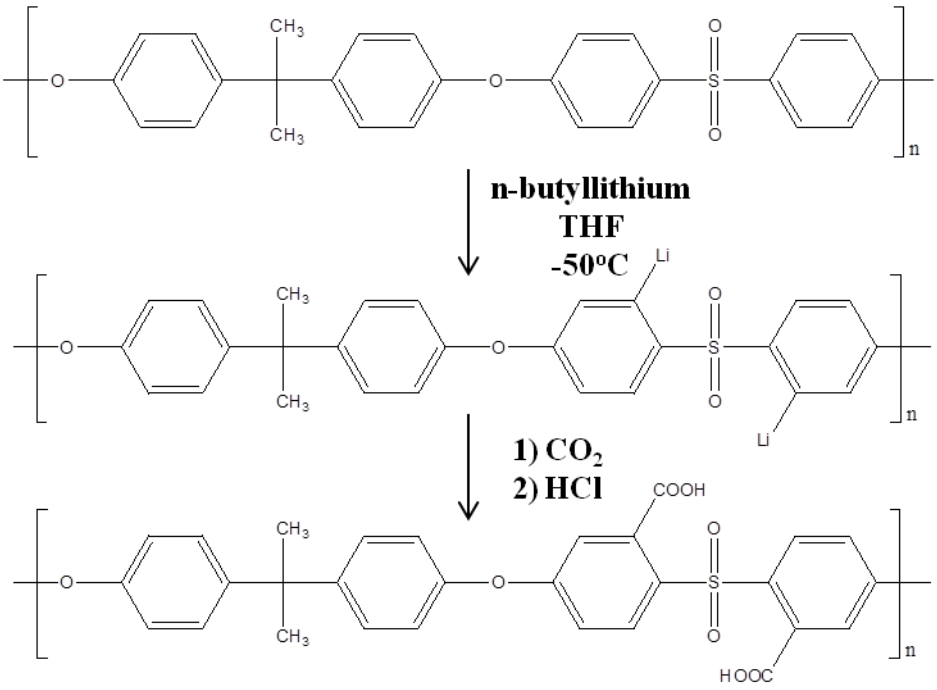

Fig. 1 (Y. H. Cho et al.)

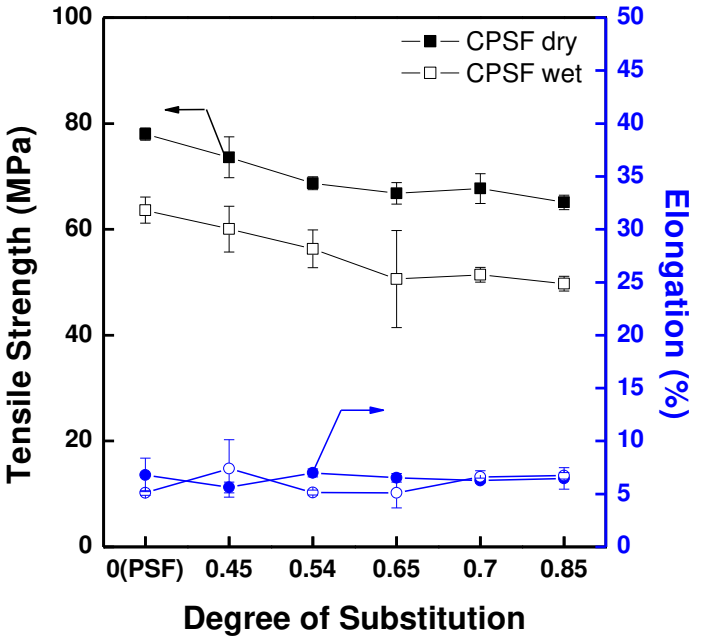

(a)

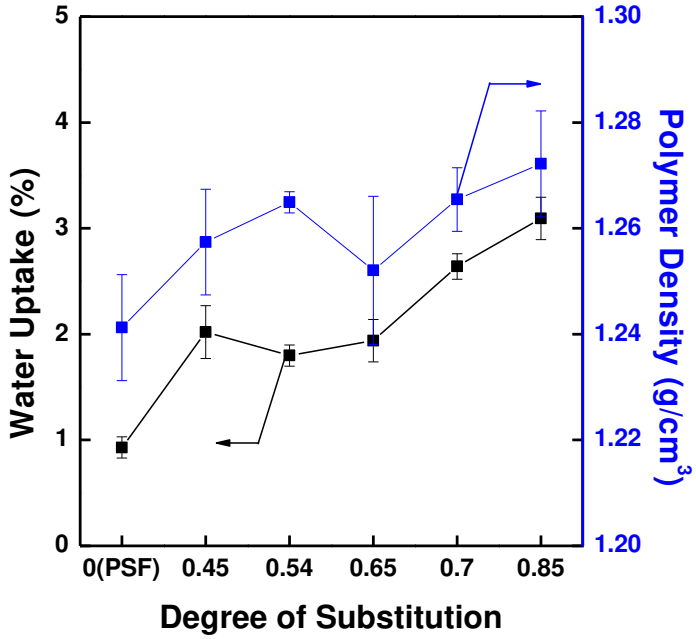

(b)

Fig. 2 (Y. H. Cho et al.)

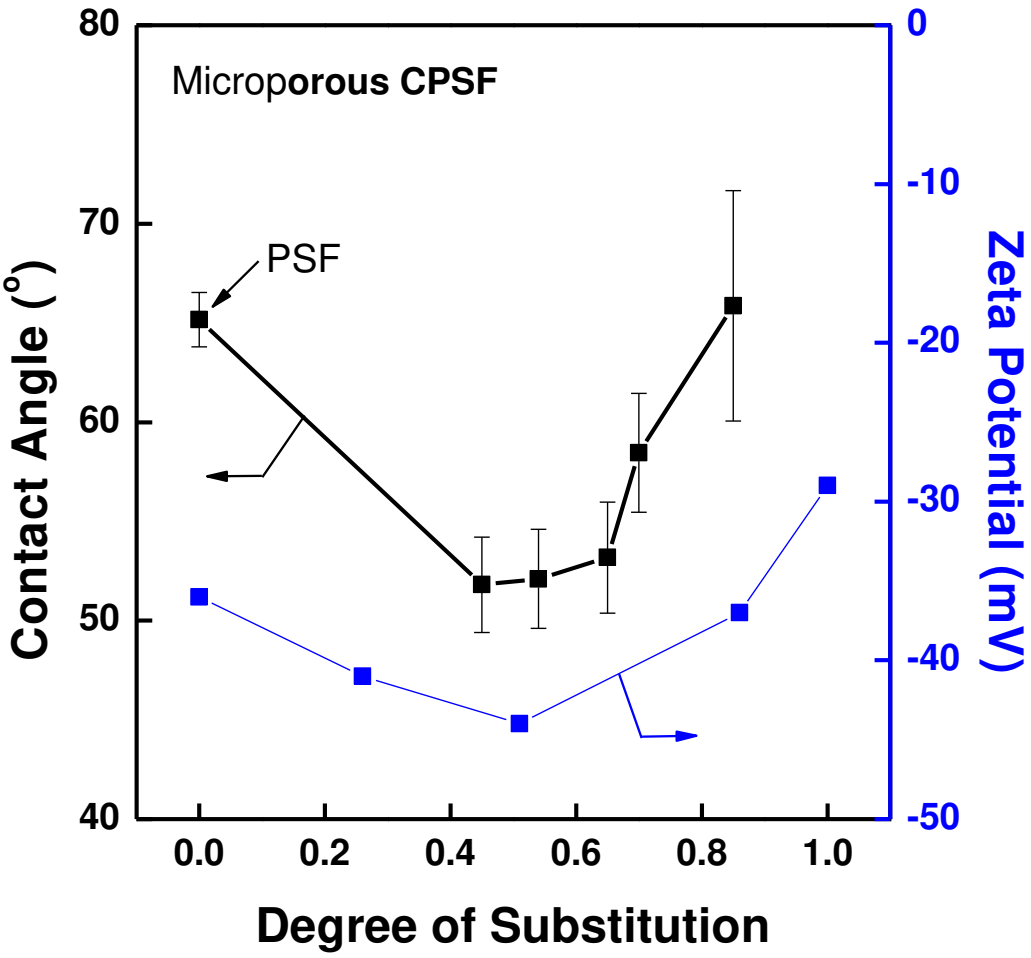

Fig. 3 (Y. H. Cho et al.)

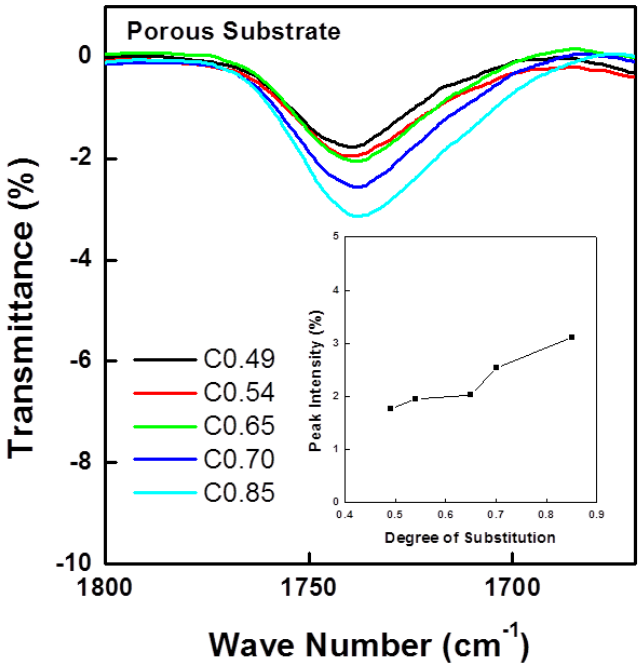

(a)

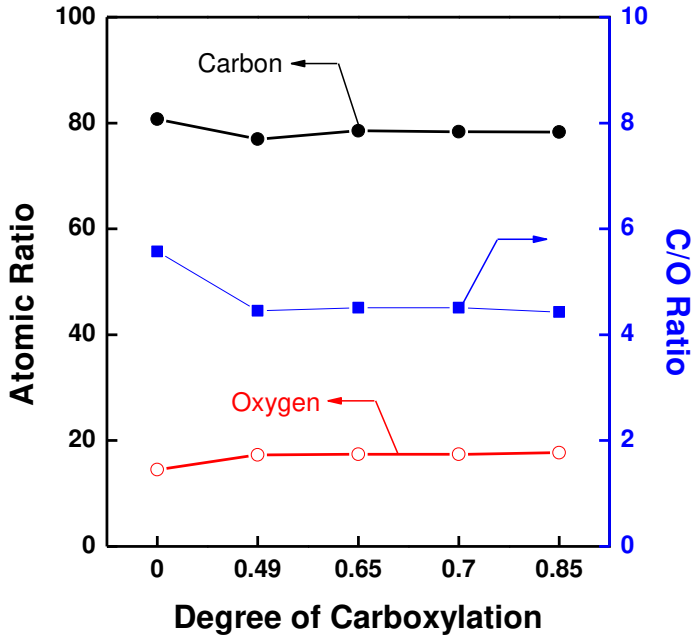

(b)

Fig. 4 (Y. H. Cho et al.)

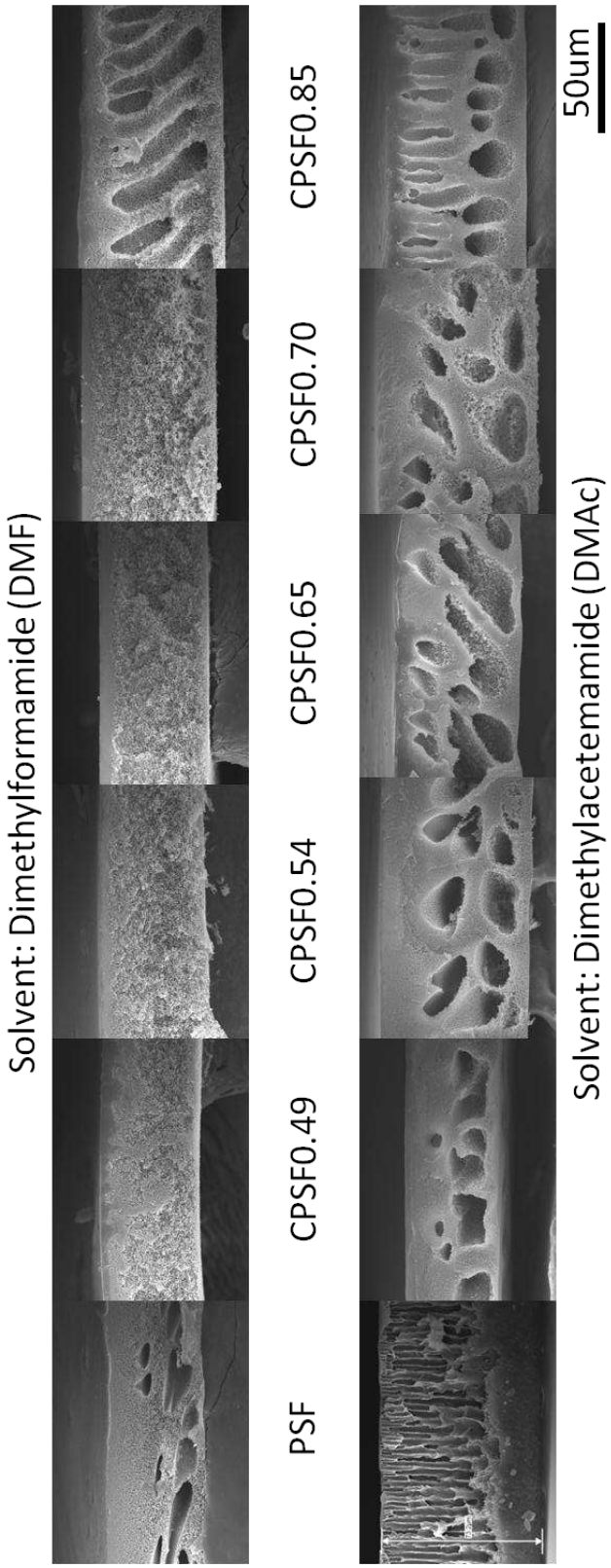

Fig. 5 (Y. H. Cho et al.)

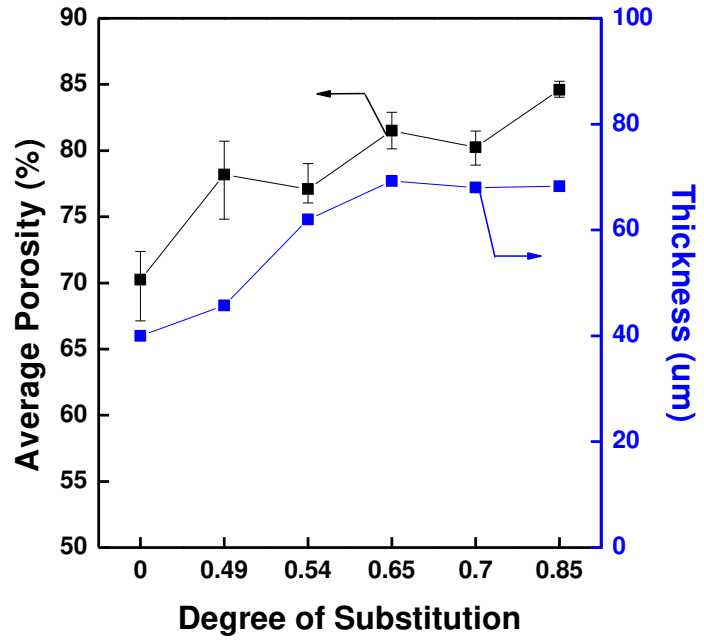

(a)

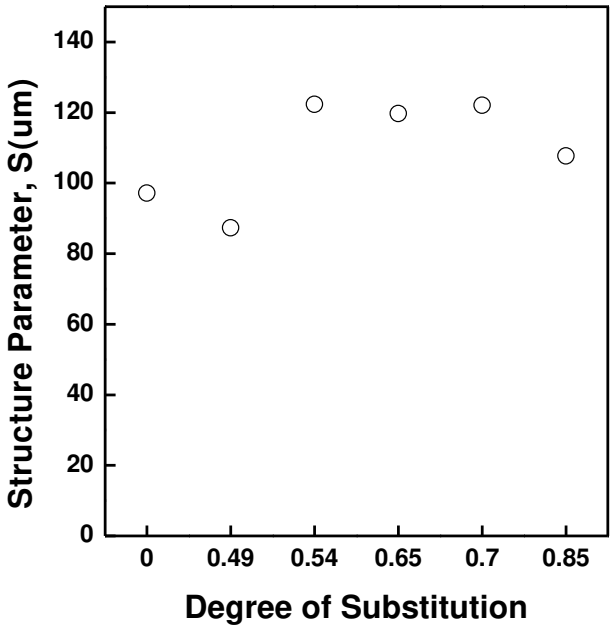

(b)

Fig. 6 (Y. H. Cho et al.)

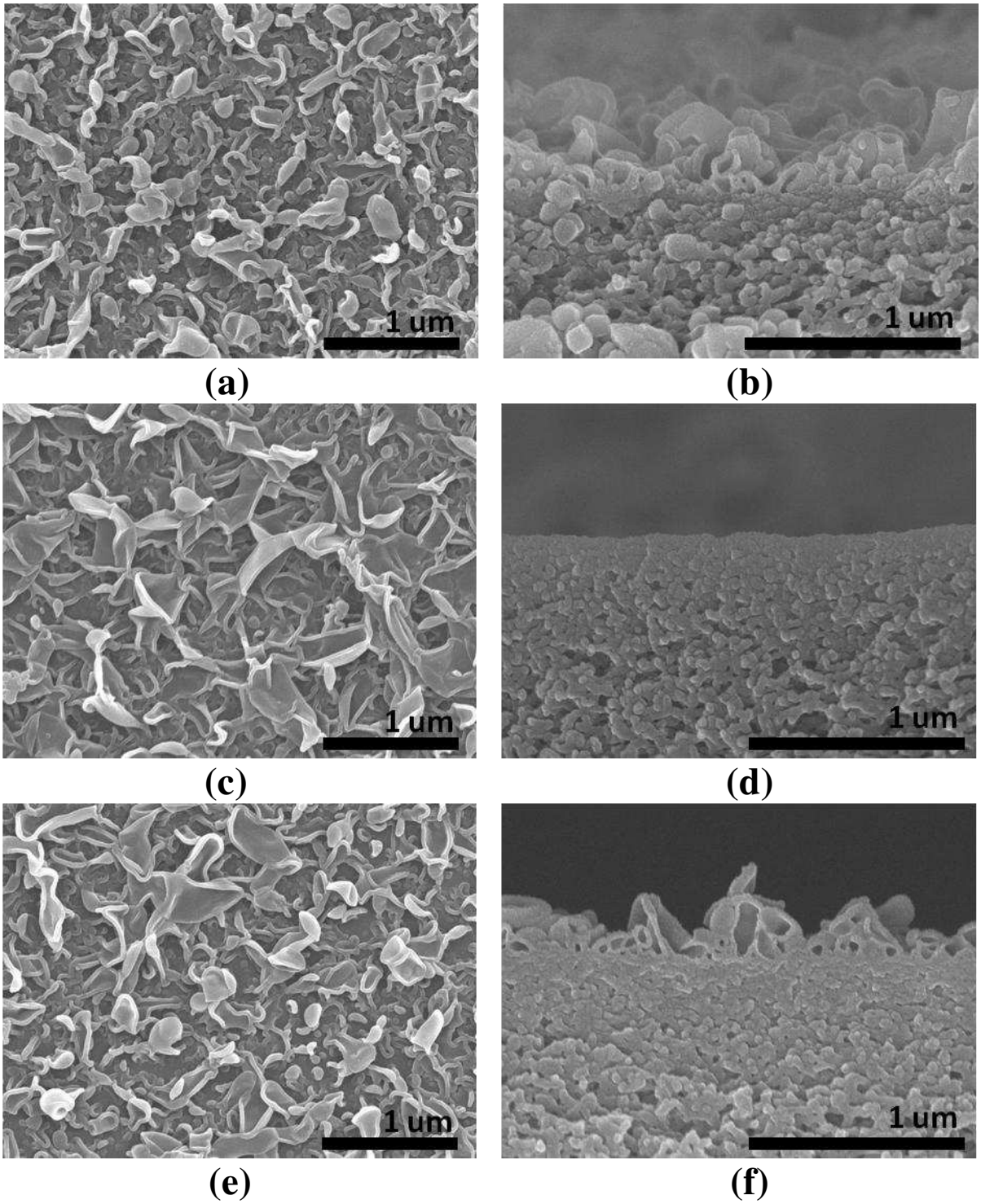

Fig. 7 (Y. H. Cho et al.)

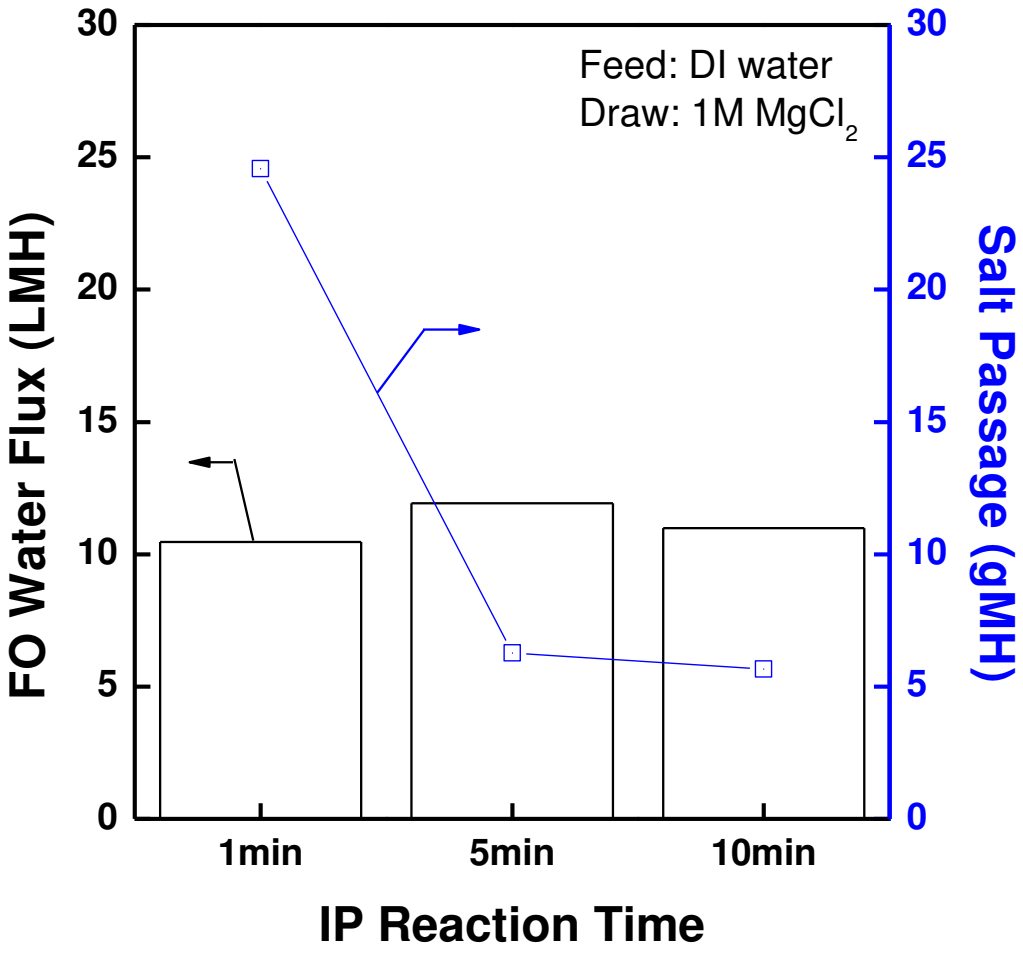

Fig. 8 (Y. H. Cho et al.)

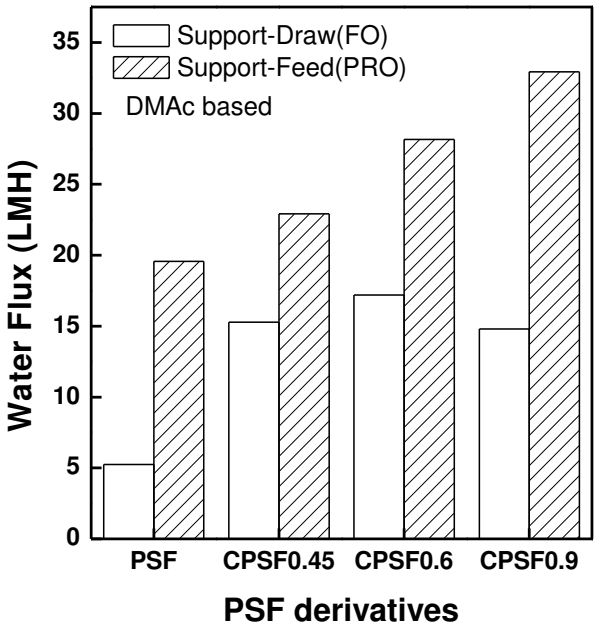

(a)

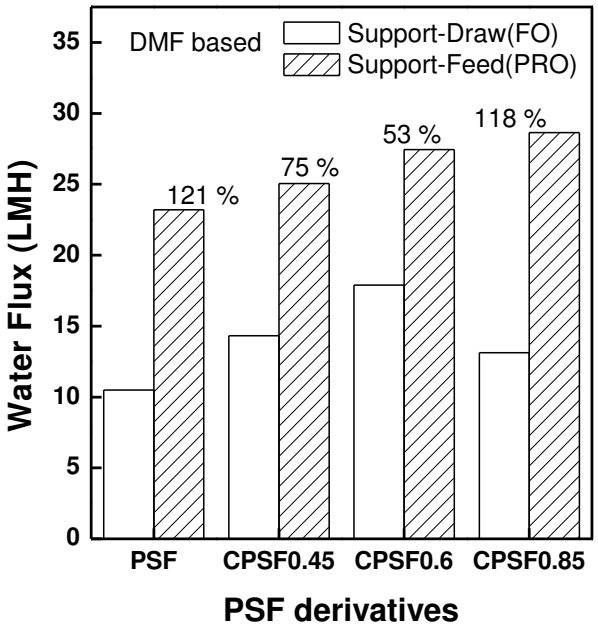

(b)

Fig. 9 (Y. H. Cho et al.)

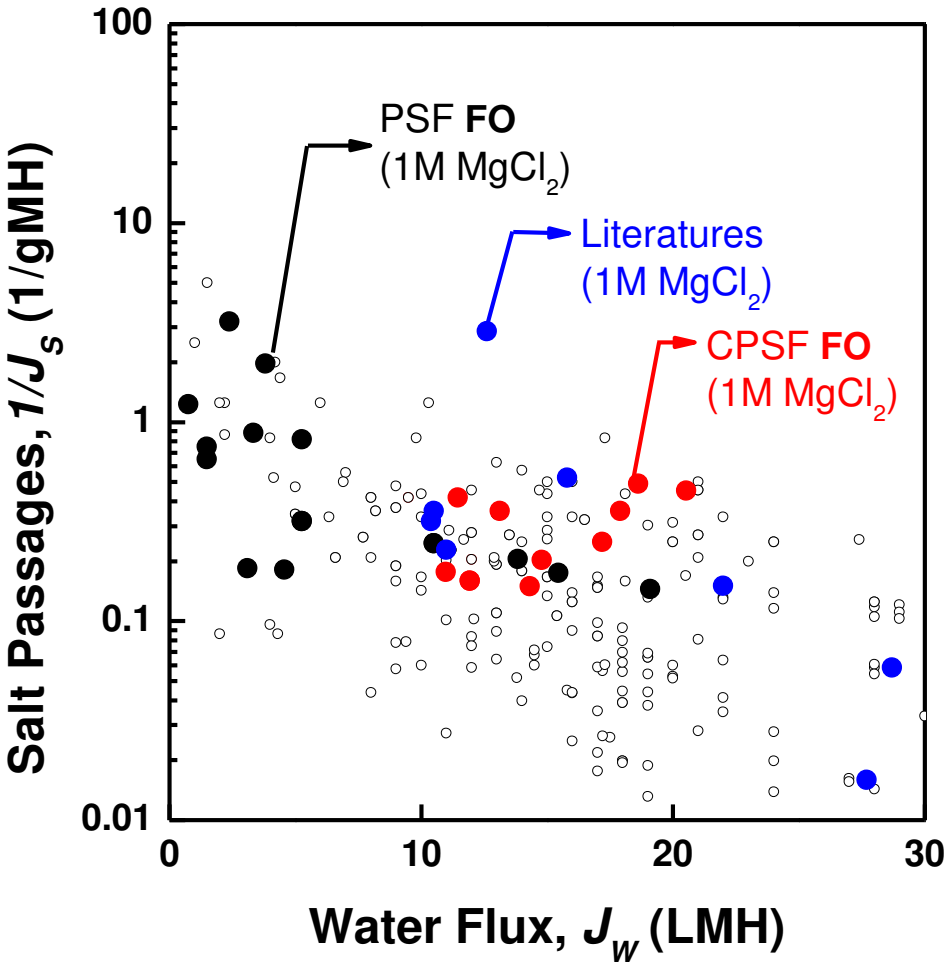

Fig. 10 (Y. H. Cho et al.)

Table 1. Comparison of water fluxes of CPSF support layers* and FO, PRO water fluxes of PA-CPSF TFC membranes

	PSF	CPSF0.45	CPSF0.6	CPSF0.85
Water flux** (LMH/bar)	500	3500	2500	2000
FO flux*** (LMH)	10.5	14.3	17.9	13.1
PRO flux*** (LMH)	23.2	25.1	27.5	28.6

***** Polymer concentration: 15 wt% in DMF, membranes were cast on glass plates and directly immersed in water coagulation bath.

** Test condition: dead-end filtration at 25°C and 1 bar; deionized water was used as feed solution

*** Test condition: cross-flow FO measurement, feed solution: D.I. water, draw solution: 1 M $MgCl_2$